# Hydrogen evolution in alkaline water on cobalt electrodeposits prepared from baths containing different anions

C. L. FAN, D. L. PIRON, H. J. MIAO, M. ROJAS

*Département de métallurgie et de génie des matériaux, École Polytechnique, Case postale 6079, succ. A, Montréal, Québec, Canada H3C 3A7*

Electrolytic cobalt deposits, as electrocatalytic materials, were prepared from baths containing chloride, sulphate or acetate. Electrodeposition was conducted at $200\,A\,m^{-2}$ with or without oxygen bubbling at the cathode. The hydrogen evolution reaction (h.e.r.) on the cobalt electrodes was performed in 30 wt % KOH at 25, 40, 50, 60 and 70 °C. Without oxygen bubbling during deposition, the cobalt electrodes prepared from the acetate bath gave superior performance for h.e.r. than electrodes deposited from the other baths. With oxygen bubbling, however, the lowest h.e.r. overpotential was obtained on the cobalt prepared from the chloride bath.

## 1. Introduction

In a previous study [1], it was shown that the h.e.r. in both alkaline and acid solutions on electrodeposited cobalt materials can be enhanced by conducting cobalt deposition with oxygen bubbling in a chloride bath. With oxygen bubbling, oxygen reduction takes place through the formation of $HO_2^-$ and $OH^-$, and cobalt hydroxide is first produced at the electrode due to the pH increase, then oxidized to cobalt oxides by the hydrogen peroxide ions [2, 3]. Cobalt is deposited through the reduction of cobalt oxides and $Co^{2+}$ ions [3]. The formation and reduction of the cobalt oxides results in porous cobalt deposits with high surface area [4]. The presence of appropriate anions may also activate dissolution of the freshly deposited metal, or metal oxides, and increase deposit porosity [2]. The catalytic performance was investigated on nickel and cobalt materials deposited from baths containing various anions [5, 6]. Khalil [5] reported that the catalytic activity for decomposition of a 0.4% $H_2O_2$ solution, calculated by measuring the exact concentrations of $H_2O_2$, before and after its passage over the catalytic materials, was very poor on a nickel electrode deposited from a chloride bath, as compared with those deposited from sulphate, iodide, nitrate or acetate solutions. Jiang and Tseung [6] showed that the electrochemical activity, indicated by the anodic peak current density during a polarization in 7 M KOH, was higher on cobalt electrodes deposited from a chloride bath with oxygen bubbling than on those deposited from sulphate, acetate or nitrate baths. This was attributed to the difference in surface morphology of the cobalt electrodes deposited with oxygen bubbling, which was directly related to the nature of solution anions.

The present study was conducted to investigate the catalytic behaviour for h.e.r., in alkaline solution, of cobalt electrodes deposited from chloride, sulphate or acetate baths. Cobalt deposition was carried out in the presence and absence of oxygen bubbling. The overpotential for h.e.r. in 30 wt % KOH at different temperatures was determined. The relationships between h.e.r. electrocatalytic performance of the cobalt deposits, their surface morphology, composition and crystalline structure and the cobalt deposition conditions were examined.

## 2. Experimental details

### 2.1. Fabrication of cobalt electrodes

The substrates used were rolled copper sheets (0.1 mm thick). Before deposition, the samples ($1.0 \times 1.0\,cm^2$) were electropolished in 2 M $H_2SO_4$ at an anodic current density of $150\,Am^{-2}$ and 25 °C for 10 min. The deposition was operated in a 1 $dm^3$ cell, and a cobalt anode was used. Each deposition was carried out at $200\,A\,m^{-2}$ and 25 °C for 1 h, and the cobalt loading on each electrode was about $20\,mg\,cm^{-2}$. For deposition with oxygen bubbling, the gas was fed through a sintered glass plug into the solution for 1 h before deposition, and was continuously fed onto the cathode during deposition at a constant rate of $230\,ml\,min^{-1}$. The bath compositions are listed in Table 1. To examine the cobalt electrodeposition kinetics, cathodic polarization was conducted by cathodic scanning at $1\,mV\,s^{-1}$.

### 2.2 Characterization of the electrolytic cobalt

Hydrogen evolution on the cobalt electrodes was examined in 30 wt % KOH at 25, 40, 50, 60 and 70 °C. Cathodic polarization of the cobalt electrodes

*Table 1. Composition of cobalt plating solutions.*

| 1. CoCl$_2$ · 6H$_2$O | 48 g dm$^{-3}$ (0.2 M) |
|---|---|
| KCl | 29 g dm$^{-3}$ (0.4 M) |
| pH | 5.6 |
| 2. CoSO$_4$ · 7H$_2$O | 56 g dm$^{-3}$ (0.2 M) |
| K$_2$SO$_4$ | 35 g dm$^{-3}$ (0.2 M) |
| pH | 3.6 |
| 3. (CH$_3$COO)$_2$Co · 4H$_2$O | 50 g dm$^{-3}$ (0.2 M) |
| CH$_3$COOK | 39 g dm$^{-3}$ (0.4 M) |
| pH | 7.4 |

was performed at a scan rate of 1 mV s$^{-1}$ in a cell connected to a potentiostat (EG&G Princeton Applied Research, Model 173). A platinum auxiliary electrode was used. A saturated calomel electrode (SCE) was immersed as a reference in the upper section of a Luggin capillary. The end of the capillary was placed close to the cobalt electrode (< 2 mm) to minimize errors due to ohmic drop, and no correction for *IR* was made. Each measurement was conducted within 10 min. The h.e.r. overpotential was determined for each cobalt electrode by comparing h.e.r. potential at a current density of 1000 A m$^{-2}$ and the calculated hydrogen equilibrium potential at each temperature. The potential variation of the reference electrode with temperature was included in the calculation. The current density at a h.e.r. overpotential of −200 mV ($i_{200}$) for each electrode at different temperatures was used to estimate the apparent activation energy. The reproducibility of the h.e.r. overpotential and current density measurements was examined by repetition of the measurements. Under comparable experimental conditions, no significant difference was found between the results of the two tests.

The time effect on the h.e.r. overpotential in 30 wt % KOH was evaluated for the cobalt electrodes deposited with oxygen bubbling. With a constant cathodic current density of 1000 A m$^{-2}$, the h.e.r. potential was monitored for 45 h by means of a recorder (Linear, model 0595-0000).

A.c. impedance measurements were conducted on the surface (apparent area: 1 cm$^2$) of the cobalt electrodes in 30 wt % KOH at 25 °C with an applied potential of −1.5 V vs SCE. At this potential, vigorous hydrogen evolution occurred; the cathodic current density was in the range 500–3000 A m$^{-2}$. The measurements were performed using a computer-controlled potentiostat (EG&G Princeton Applied Research, model 273) in combination with a phase lock-in analyser (EG&G Princeton Applied Research, model 5208). A small a.c. voltage with an amplitude of 5 mV was superimposed on the applied potential in the frequency range 5 Hz–10 kHz. The characteristic behaviour of a single *R*–*C* combination was found from impedance spectra. The apparent double-layer capacity ($C_{dl,app}$) was evaluated from the impedance response for each electrode, according to the measured charge transfer resistance and critical frequency. The surface roughness factor for a porous electrode was thus calculated by dividing the $C_{dl,app}$ value by the double-layer capa-

city (20 $\mu$F cm$^{-2}$) for a smooth mercury electrode [2]. The inhomogeneity at the rough surface may produce frequency dependence of the double layer capacity [7]. To explain this phenomenon, a fractal surface model was developed and a so-called constant phase element (CPE) was assumed to replace the double layer capacity [8, 9]. However, this model has been criticized [10, 11], and further investigation is required. The surface roughness factors are considered to be proportional to electrode surface areas, and can be compared for the surface areas.

The surface morphology of the cobalt electrodes before polarization was observed using SEM (JEOL,JSM-820). The composition and preferred orientation of the cobalt deposits were examined by means of X-ray diffraction (X-ray diffractometer: Philips PW 1130) with copper $K_{\alpha 1}$ radiation ($\lambda = 0.15405$ nm). The preferred crystalline orientations and corresponding texture coefficients of the cobalt deposits were determined using a method reported in the literature [12].

## 3. Results

Figure 1 shows the polarization curves for cobalt electrodeposition without oxygen bubbling. The controlling step may be changed by conducting the depositions at different current densities. When deposition is carried out at a current density less than 100 A m$^{-2}$ in the test range, the relationship between deposition potential and density is linear on a semilog graph, as predicted by the Tafel law for activation-control. As the deposition current density increases beyond this range, deposition is increasingly affected by the diffusion of cations towards the cathode. The limiting current density is approximately 200 A m$^{-2}$ in the acetate bath and 300 A m$^{-2}$ in the chloride and sulphate baths, respectively.

Table 2 lists the h.e.r. overpotentials ($-\eta$: deposition with oxygen bubbling, and $-\eta'$: deposition without oxygen bubbling) in 30 wt % KOH at 25 °C on the cobalt electrodes. Without oxygen bubbling, the cobalt deposited from the acetate bath shows a lower
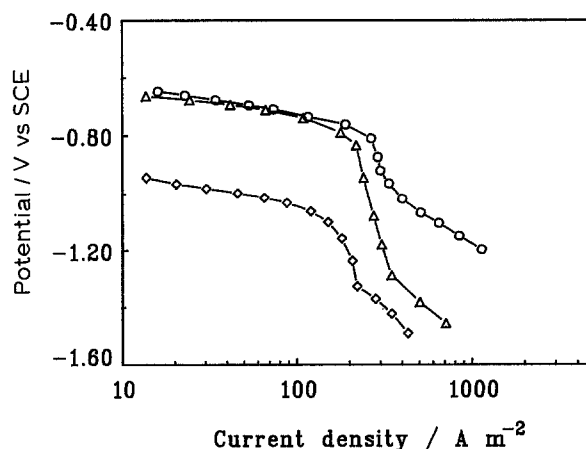


Fig. 1. Polarization of the cobalt electrodeposition in different baths without oxygen bubbling, scan rate: 1 mV s$^{-1}$, 25°C. (○) Chloride, (△) sulphate, (◇) acetate.

Table 2. H.e.r. overpotential at $1000\,A\,m^{-2}$ in 30 wt % KOH at 25 °C on cobalt electrodes prepared from baths containing different anions.

| Bath | $-\eta'/mV$ | $-\eta/mV$ | $[(-\eta')-(-\eta)]/(-\eta')$ |
|------|------|------|------|
| Chloride | 374 | 293 | 0.22 |
| Sulphate | 461 | 383 | 0.17 |
| Acetate | 332 | 314 | 0.05 |

$\eta'$: h.e.r. overpotential on Co, deposition without oxygen bubbling.
$\eta$: h.e.r. overpotential on Co, deposition with oxygen bubbling.

h.e.r. overpotential than that from the chloride and sulphate baths. The highest overpotential is obtained on the cobalt prepared from the sulphate bath. A decrease in h.e.r. potential can be achieved on the cobalt electrodes deposited with oxygen bubbling. The ratio of $[(-\eta') - (-\eta)]/(-\eta')$ characterizes the enhancement of h.e.r. on the electrodes deposited with oxygen bubbling. The decrease in overpotential is 22% and 17% for cobalt prepared from the chloride and sulphate baths, whereas, from the acetate bath, the decrease is only 5% (see Table 2). With oxygen bubbling, the cobalt deposited from the chloride bath gives the lowest h.e.r. overpotential, and the highest h.e.r. overpotential is found on that produced from the sulphate bath.

The apparent double-layer capacity and the deduced surface roughness factor of the cobalt electrodes are listed in Table 3. In the case of deposition without oxygen bubbling, the surface roughness factor produced from the acetate bath is about 5 and 13 times larger than those prepared from the chloride and sulphate baths, respectively. For the deposition with oxygen bubbling, the surface roughness factor of the electrode from the chloride bath is about 1.6 and 2.8 times greater than those from the acetate and sulphate baths. A comparison in surface roughness factors can also be made for the cobalt electrodes deposited with and without oxygen bubbling during deposition. With oxygen bubbling, the surface roughness factor is about 11 times larger for the cobalt deposited from the chloride and sulphate baths, and only around 1.5 times greater for the cobalt from the acetate bath than that deposited without oxygen bubbling (see Table 3). The scanning electron micrographs (see Fig. 2) show the surface morphology of the deposits. From a deposition without bubbling oxygen, the structure of the cobalt prepared from

Table 3. $C_{dl,app}$ and surface roughness factor of the cobalt electrodes deposited from different baths

| Bath | $C_{dl,app}/\mu F\,cm^{-2}$ | | Surface roughness factor | |
|------|------|------|------|------|
| | a | b | a | b |
| Chloride | 3173 | 34 522 | 159 | 1726 |
| Sulphate | 1111 | 12 316 | 56 | 616 |
| Acetate | 14 360 | 22 078 | 718 | 1104 |

a Cobalt deposition without oxygen bubbling.
b Cobalt deposition with oxygen bubbling.

the chloride and sulphate baths is relatively compact with respect to that from the acetate bath (see Fig. 2(a), (c) and (e)). As the deposition is conducted with oxygen bubbling, the structure of the cobalt from the chloride and sulphate baths becomes significantly looser (compare Fig. 2(a) and (b), (c) and (d)); however, no significant difference in surface morphology on the cobalt deposited from the acetate solution was found, with respect to the deposition without oxygen bubbling (compare Fig. 2(e) and (f)).

The h.e.r. overpotential $(-\eta)$ of the cobalt deposits in 30% KOH at different temperatures is presented in Fig. 3. The deposits were prepared from the different baths in the presence of oxygen bubbling. For all the baths, a decrease in h.e.r. overpotential with increasing temperature occurs. At a comparable temperature, the h.e.r. overpotential on the cobalt from the chloride bath is lower than those from the sulphate and acetate baths. The overpotential on the cobalt from the sulphate bath has the highest value (see Fig. 3). Figure 4 shows the Arrhenius plot of $\log(i_{200})$ against $T^{-1}$ for the cobalt electrodes. The apparent activation energy has a value of 82, 84 and $85\,kJ\,mol^{-1}$ for the cobalt deposited from the chloride, sulphate and acetate baths, respectively.

The time variation effect on the h.e.r. overpotential in 30 wt % KOH at 25 °C is illustrated in Fig. 5 for the cobalt electrodes deposited with oxygen bubbling. For the cobalt prepared from the chloride and sulphate baths, the overpotential $(-\eta)$ initially decreases with time during the first 30–40 h. Then the overpotential becomes constant; the decrease in the h.e.r. overpotential is about 80 mV. For the cobalt deposited from the acetate bath, however, no significant change can be seen in the h.e.r. overpotential over the entire time range. The h.e.r. overpotential on the cobalt electrode deposited from the chloride bath is obviously lower than on those from the sulphate and acetate baths (see Fig. 5).

The composition, preferred orientation and texture coefficient of the cobalt deposited from the different baths are presented in Table 4. The deposits prepared from all the baths without oxygen bubbling were composed only of cobalt. With oxygen bubbling, not only cobalt, but also a trace of $\alpha$-$Co(OH)_2$ were detected in the deposits produced from the chloride and sulphate baths; however, the deposit prepared from the acetate bath only contained cobalt. The preferred orientations of the hexagonal cobalt deposited from the chloride and acetate baths are the same, namely [1 0 2] and [1 0 0] for the deposition without oxygen bubbling, and [1 0 2], [1 0 0] and [1 0 1] (slightly) with oxygen bubbling. For the hexagonal cobalt deposited from the sulphate bath, the preferred orientation is only [1 0 0] (see Table 4).

## 4. Discussion

### 4.1. Effect of surface area

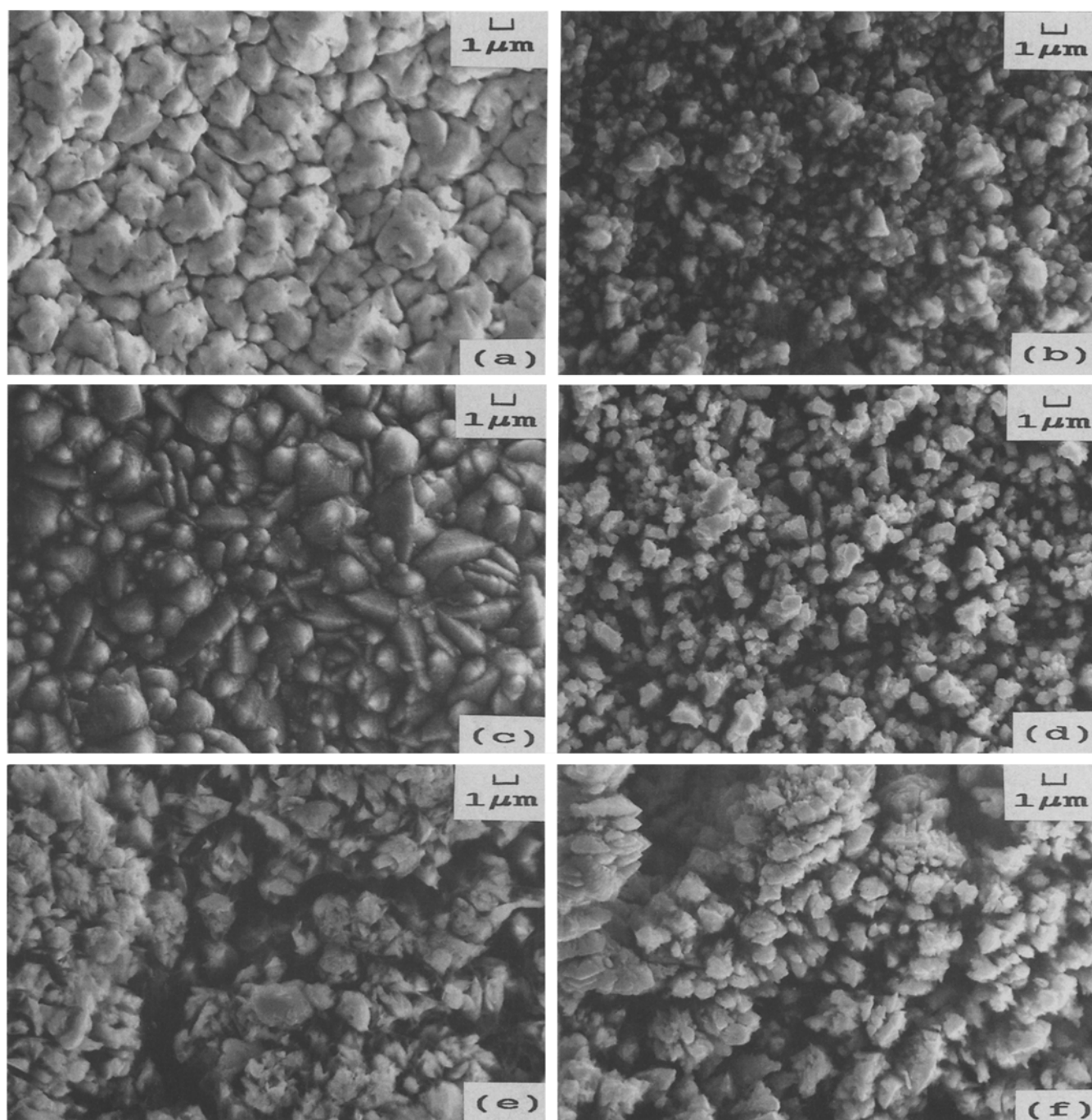The effect of surface area on h.e.r. catalytic per-

Fig. 2. Scanning electron micrographs showing surface morphology of the cobalt electrodes deposited from different baths with or without oxygen bubbling, oxygen flow rate: 230 ml min$^{-1}$, current density: 200 A m$^{-2}$, 25 °C; (a) chloride bath, no oxygen bubbling; (b) chloride bath, with oxygen bubbling; (c) sulphate bath, no oxygen bubbling; (d) sulphate bath, with oxygen bubbling; (e) acetate bath, no oxygen bubbling; (f) acetate bath, with oxygen bubbling.

formance is clearly shown on the cobalt electrodes prepared from the baths containing different anions. Without oxygen bubbling during deposition, the cobalt produced from the acetate bath shows the lowest h.e.r. overpotential (see Table 2). With the acetate solution, the deposition current density used (200 A m$^{-2}$) is just the limiting current density (Fig. 1). The deposition is controlled by the mass transport of cations towards the cathode. Consequently, the initial roughness of the electrode is amplified and the electrode surface is rather rough and porous [1] (Fig. 2(e)). The surface area of the electrode is thus considerably enlarged with respect to the apparent surface area (Table 3). For the electrodes prepared

from the chloride and sulphate baths, the used deposition current density is significantly lower than the limiting current density (300 A m$^{-2}$), and the increase in the electrode surface is much less. The h.e.r. overpotential on these electrodes is thus higher.

On the cobalt deposited from the chloride and sulphate baths, oxygen bubbling during deposition results in an apparent decrease in h.e.r. overpotential. However only a slight decrease in h.e.r. overpotential is achieved on the cobalt deposited from the acetate bath with oxygen bubbling (Table 2). From the chloride and sulphate baths, the cobalt surface becomes much more porous with than without oxygen bubbling (Fig. 2), and the surface area is
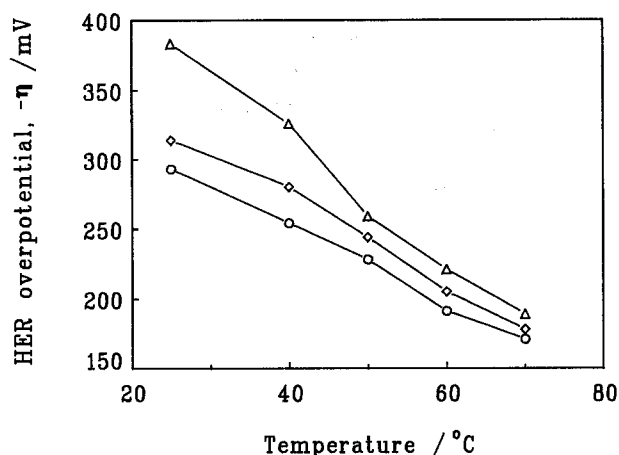
Fig. 3. H.e.r. overpotential (at a current density of $1000 \, A \, m^{-2}$) in 30 wt % KOH at different temperatures on the cobalt electrodes deposited from different baths with oxygen bubbling, deposition current density: $200 \, A \, m^{-2}$, oxygen flow rate: $230 \, ml \, min^{-1}$, 25 °C. ($\triangle$) Sulphate, ($\Diamond$) acetate, ($\bigcirc$) chloride.
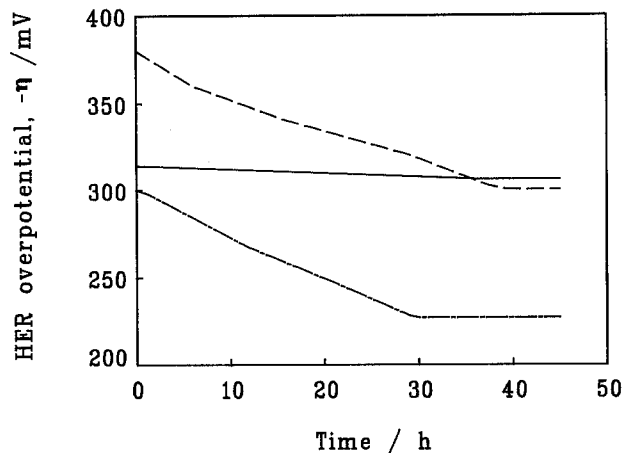


Fig. 5. Time effect on the h.e.r. overpotential at $1000 \, A \, m^{-2}$ in 30 wt % KOH at 25 °C for the cobalt electrodes deposited from different baths with oxygen bubbling, deposition current density: $200 \, A \, m^{-2}$, oxygen flow rate: $230 \, ml \, min^{-1}$, 25 °C. (– – –) Sulphate, (——) acetate, (– – – – –) chloride.

extensively enlarged (Table 3). From the acetate bath, however, no significant difference is found in the surface morphology on the cobalt electrodes with and without oxygen bubbling during deposition (Fig. 2(e) and Fig. 2(f)); and the surface roughness factor is only slightly increased (Table 3). After deposition with oxygen bubbling, cobalt hydroxide is detected on the deposits produced from the chloride and sulphate baths, but not on that from the acetate bath (Table 4). This is in agreement with the previous research of Jiang *et al.* [13]. They determined the mechanism and kinetics of cobalt electrodeposition with oxygen dissolved in chloride, sulphate and acetate baths. In the chloride and sulphate baths, a

large portion of the cobalt hydroxide at the electrode surface is oxidized by hydrogen peroxide, forming various cobalt oxides. The formation and reduction of cobalt oxides results in a much more porous deposit than that prepared without oxygen. In the acetate bath with oxygen, however, there is much less cobalt hydroxide at the electrode, and oxygen is predominantly reduced to produce water instead of hydrogen peroxide. Consequently, the deposit is not considerably more porous than that produced without oxygen. The activation effect of chloride ions on oxide reduction during cobalt deposition was confirmed by a cyclic voltammetry study carried out in various solutions with oxygen bubbling [6].

### 4.2. Effect of composition, structure and test temperature

The composition and crystallographic planes of the electrode surface may also exert an impact on its catalytic performance. Okuyama *et al.* [14] observed an increase in h.e.r. activity of the niobium electrode in 25 wt % KOH due to a reduction in electrode surface oxide. The reduction of the cobalt hydroxide remaining
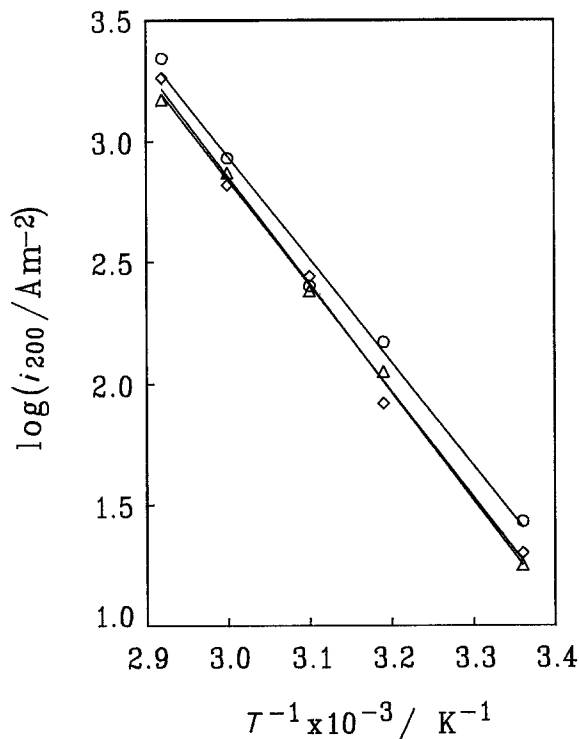


Fig. 4. Arrhenius plot for the h.e.r. in 30 wt % KOH on the cobalt electrodes deposited from different baths with oxygen bubbling, deposition current density: $200 \, A \, m^{-2}$, oxygen flow rate: $230 \, ml \, min^{-1}$, 25 °C. ($\bigcirc$) Chloride, ($\Diamond$) acetate, ($\triangle$) sulphate.

Table 4. Effect of bath composition and oxygen bubbling on the composition and preferred orientation of cobalt deposits.

| Bath | Composition | | Preferred orientation and texture coefficient | |
|---|---|---|---|---|
| | a | b | a | b |
| Chloride | Co | Co | [1 0 2] >11.0 | [1 0 2] >5.0 |
| | | $\alpha$-Co(OH)$_2$ | [1 0 0]  1.6 | [1 0 0]  4.1 |
| | | | | [1 0 1]  1.3 |
| Sulphate | Co | Co | [1 0 0]  7.9 | [1 0 0]  7.3 |
| | | $\alpha$-Co(OH)$_2$ | | |
| Acetate | Co | Co | [1 0 2] >7.0 | [1 0 2] >6.0 |
| | | | [1 0 0]  3.4 | [1 0 0]  4.7 |
| | | | | [1 0 1]  1.4 |

a Cobalt deposition without oxygen bubbling.
b Cobalt deposition with oxygen bubbling.

on the cobalt deposited from the chloride and sulphate baths with oxygen bubbling could also result in an improvement of the h.e.r. in alkaline water electrolysis. During the time test, the cobalt hydroxide could have been gradually reduced and dissolved, the activity of the electrode could have increased, thus lowering the h.e.r. overpotential. After reduction, the h.e.r. overpotential on the electrode remained constant (Fig. 5). The electrode prepared from the acetate bath is composed only of cobalt, and no improvement on the h.e.r. is achieved during the time test. The improved h.e.r. on the electrodes deposited from the chloride bath as compared with those from the sulphate solution could be attributed not only to the effect of electrode surface area but also to the variation in the preferred crystalline orientations of the electrodes produced from the different baths. The preferred [1 0 2] and [1 0 1] planes in the cobalt from the chloride bath would be favourable to the h.e.r. in water electrolysis (Table 4).

The h.e.r. in alkaline water on the cobalt electrodes can be enhanced as the test temperature increases (Fig. 3). This is consistent with the results obtained on other electrocatalytic materials [15,16]. The deduced apparent activation energy (around $84\,kJ\,mol^{-1}$) for the h.e.r. on the cobalt electrodes is on the same order of magnitude, but higher than those reported previously for nickel-based catalytic materials, such as $24\,kJ\,mol^{-1}$ on Ni–Sn alloys [15]. No data of the apparent activation energy on cobalt electrodes has been reported in the literature.

## 5. Conclusions

The h.e.r. in the electrolysis of 30 wt % KOH alkaline water on electrodeposited cobalt can be promoted via an increase in electrode surface area by conducting the deposition at the limiting current density and by oxygen bubbling during deposition. An improvement in surface activity for h.e.r. of cobalt electrodes is achieved following cathodic activation for 30–40 h in alkaline solution, possibly due to the reduction of cobalt hydroxide remaining on the electrodes. The variation in preferred orientation of the cobalt deposits may affect the catalytic performance for h.e.r. in water electrolysis. An increase in temperature during water electrolysis results in a decrease in h.e.r. overpotential on the cobalt electrodes.

## References

[1]   M. Rojas, C. L. Fan, H. J. Miao and D. L. Piron, *J. Appl. Electrochem.* **22** (1992) 1135.
[2]   S. P. Jiang, Y. Z. Chen, J. K. You, T. X. Chen and A. C. C. Tseung, *J. Electrochem. Soc.* **137** (1990) 3374.
[3]   S. P. Jiang and A. C. C. Tseung, *ibid.* **137** (1990) 3381.
[4]   C. Q. Cui, S. P. Jiang and A. C. C. Tseung, *ibid.* **139** (1992) 60.
[5]   R. M. Khalil, *J. Appl. Electrochem.* **18** (1988) 292.
[6]   S. P. Jiang and A. C. C. Tseung, *J. Electrochem. Soc.* **137** (1990) 3387.
[7]   R. De Levie, *Electrochimica Acta* **10** (1965) 113.
[8]   L. Nyikos amd T. Pajkossy, *ibid.* **30** (1985) 1533.
[9]   W. H. Mulder and J. H. Sluyters, *ibid.* **33** (1988) 303.
[10]  J. C. Wang, *ibid.* **33** (1988) 707 and **34** (1989) 987.
[11]  R. De Levie, *J. Electroanal. Chem.* **261** (1989) 1.
[12]  L. Ph. Bérubé and G. L'Espérance, *J. Electrochem. Soc.* **136** (1989) 2314.
[13]  S. P. Jiang, C. Q. Cui, A. C. C. Tseung, *ibid.* **138** (1991) 3599.
[14]  M. Okuyama, G. Bélanger and D. L. Piron, *Int. J. Hydrogen Energy* **3** (1978) 297.
[15]  A. Bélanger and A. K. Vijh, *ibid.* **12** (1987) 227.
[16]  I. Arul Raj and V. K. Venkatesan, *ibid.* **13** (1988) 215.